Proceedings of the Seventh International Conference on
Railway Technology: Research, Development and Maintenance
Edited by: J. Pombo
Civil-Comp Conferences, Volume 15, Paper 10.13
Civil-Comp Press, Edinburgh, United Kingdom, 2026
ISSN: 2753-3239, doi: 10.4203/ccc.15.10.13


# Influence of Overlap Section Design on Dynamic Interaction of Multiple Pantographs with High-Speed Catenary System

**M. Mohammadpour, V. Bokaeian and F. Vesali**

**Simulation Group, PANTOhealth GmbH,
Berlin, Germany**

## Abstract

The overlap section of high-speed railway catenary is one of the most critical area for current collection quality, especially when more than one pantograph is collecting current from same catenary. In this paper, the dynamic interaction between four pantographs and a two-section catenary with one overlap is studied by means of numerical simulation through PANTOsim. Three different overlap profiles are used and compared at five operating speeds from 250 to 350 km/h. The standard deviation of contact force is used as the main criterion of the contact quality assessment. The results indicates that the third profile gives the best dynamic behaviour, in particular at 275 km/h, where the standard deviation of contact force is much smaller than for the other two profiles. Furthermore, twelve different distance scenarios between pantographs were investigated, by considering the wavelength of the pantograph induced vibrations in the catenary system. The combination of distances $d_1$=192 m, $d_2$=120 m, $d_3$=192 m (Scenario 9) shows good compliance with EN 50367 for all four pantographs. The presented work demonstrates that the geometric design of the overlap, together with proper choice of distance between pantographs, can reduce strongly the contact force fluctuation and therefore improve the wear of contact wire.

**Keywords:** pantograph-catenary interaction, overlap section, multiple pantographs, contact force, EN 50318, PANTOsim.

## 1 Introduction

The pantograph-catenary system is the only one practical solution that has been used until now for transmitting electrical energy from the fixed infrastructure to the moving train. The quality of this interaction has a strong influence not only on the reliability of the electrical supply, but also on the maintenance cost of both pantograph head and contact wire. When the train speed increases, the dynamic behaviour of the system became more complex, and the contact force show large oscillations which may cause loss of contact, electric arcs and accelerate wear of the carbon strip and the contact wire.

In modern high-speed lines, it is common to find multiple unit trains with two pantographs raised, or two locomotives coupled together with up to four active pantographs. In this configuration, the leading pantograph excites the contact wire, and the propagated waves arrive at the trailing pantograph before they are damped out. Because of this reason, the trailing pantograph operates in a perturbed catenary state, and its contact force quality is generally worse than the leading one. Bruni et al. [1] presented the benchmark of pantograph-catenary interaction simulation codes, where ten different commercial and research codes are compared on a reference catenary. The benchmark concludes that the agreement between codes is good for single pantograph, but the dispersion increases when multiple pantographs are simulated. Ambrosio et al. [2] proposed a co-simulation procedure between multibody dynamics of the pantograph and finite element model of the catenary. Their work shows that the irregular geometry at the overlap may produce very high force peaks if the transition is not designed carefully. Pombo and Ambrosio [3] investigated the effect of distance between two pantographs on the contact force of trailing one. They reported that for distances near to one and two times of the span length the trailing pantograph has the highest standard deviation. Liu et al. [4] simulated a three-pantograph configuration on Chinese high-speed line. The second and third pantograph have respectively 25% and 38% higher standard deviation of contact force than the first one, at 350 km/h. Song et al. [5] focused on the overlap section and the geometrical. They concluded that a smooth transition of the contact wire height in the overlap region is essential to limit the impact load on the second pantograph entering the overlap. Song et al. [6] introduced an active control of pantograph head, which can compensate the contact force fluctuation generated by the overlap. Bautista et al. [7] identified that the most critical point is the second pantograph passing under the overlapping span, where two contact wires are present at the same time. Massat et al. [8] used a stochastic approach for catenary modelling. They showed that the variability of contact force is amplified by the presence of the second pantograph by a factor between 1.5 and 2. Zhang et al. [9] proposed a hybrid simulation model where the catenary is modelled by absolute nodal coordinate formulation (ANCF). They concluded that the high-frequency component of the contact force, often filtered out by classical models, plays an important role in the trailing pantograph behaviour. Tan et al. [10] applied machine learning techniques to predict the contact force quality of multiple pantographs, based on operating speed, pantograph distance and catenary parameters. Vesali et al. [11] formulated the equations of motion of the catenary using Euler-Bernoulli beam theory for messenger and contact wire, with non-linear dropper elements that can only transmit tension. The same authors [12] extended the model to include the effect of pantograph head rotational degree of freedom and applied the model to estimate the contact wire wear distribution along the line. Vesali [13] in his Ph.D. thesis collected the whole formulation in a comprehensive way and validated the simulation tool against the standard EN 50318 reference case. The results match very well with the benchmark values, and the tool was later developed into the PANTOsim. Cho et al. [14] investigated the effect of stagger angle and pre-sag on the contact force in Korean high-speed catenary. Their result shows that pre-sag of 1/2000 of span length give the best compromise between current collection quality and contact wire uplifting.

From this literature review, the overlap region together with the distance between pantographs in multi-pantograph operation are still open questions. Most of the existing works' analyses either the overlap design or the pantograph distance, but rarely both effects together with realistic four pantograph configurations. The present paper tries to fill this gap by simulating,

using PANTOsim, four pantographs running over a two-section catenary with one overlap, where three different overlap profiles are designed and twelve distance scenarios are analysed in respect to the EN 50318 standard.
The paper is organized as follow. Section 2 describes the modelling approach of catenary, pantograph and contact, based on the formulation of Vesali. Section 3 presents the test bench catenary system with the three overlap profiles. Section 4 discusses the simulation results in terms of standard deviation of contact force and gives the compliance of each scenario. Finally, the main conclusions and the next steps of the research are reported.

# 2 Modeling

The mathematical model adopted in this paper follow the formulation presented by Vesali in his Ph.D. thesis [13] and in the related papers [11, 12]. The same formulation is the core of the PANTOHEALTH simulation engine, which has been used to perform all the numerical analyses presented in the following sections. In this part, only the most important equations are recalled, the complete derivation can be found in the original references.

## 2.1 Catenary model

The catenary system is composed by the contact wire (CW), the messenger wire (MW), the droppers, the steady arm and the registration arm. Both contact wire and messenger wire are modelled as Euler-Bernoulli beam under axial tension. The equation of motion of the contact wire is:

$$EI\frac{\partial^4 w}{\partial x^4} - T\frac{\partial^2 w}{\partial x^2} + \rho A\frac{\partial^2 w}{\partial t^2} + c\frac{\partial w}{\partial t} = f(x,t) \quad (1)$$

where EI is the bending stiffness, T is the tension force, $\rho A$ is the linear mass density, c is the damping coefficient, $w(x,t)$ is the vertical displacement of the contact wire, and $f(x,t)$ is the external force per unit length, that include the gravity, the dropper forces and the contact force from pantograph. Similar equation is written for the messenger wire.
The droppers are modelled as non-linear spring elements which can transmit only tension force (no compression). This is fundamental property of the dropper, because the dropper is a cable, and it goes slack when the contact wire is uplifted. The dropper force is:

$$\begin{cases} F_d = k_d.(L - L_0) & if\ L > L_0 \\ F_d = 0 & if\ L \leq L_0 \end{cases} \quad (2)$$

where L is the current length of dropper and $L_0$ is the natural length. The non-linearity of the droppers is a strong source of complexity in the simulation, because the stiffness matrix changes at each time step depending on the slack/tension state of the droppers.
The supports (steady arm and registration arm) are introduced in the model as flexible attachment, with a vertical stiffness representing the bending behaviour of the bracket and the rotation of the registration arm. The stagger of the contact wire at each support is also taken into account in 3D version of the model, because it influences the longitudinal position of the contact point between pantograph and contact wire.

## 2.2 Pantograph model

The pantograph is modelled as a discrete mass-spring-damper system with three degrees of freedom, representing respectively the pantograph head (collector strip), the upper frame and the lower frame. The equation of motion of the pantograph is written as:

$$M\ddot{x} + C\dot{x} + Kx = F_s - F_c e_1 \tag{3}$$

where M, C and K are respectively the 3×3 mass, damping and stiffness matrices of pantograph, x is the displacement vector, $F_s$ is the static uplift force applied at the lower frame, $F_c$ is the contact force between collector strip and contact wire, and $e_1$ is the unit vector indicating that the contact force acts only on the first degree of freedom (the collector strip).
The contact between collector strip and contact wire is modelled with a penalty approach. A high stiffness contact spring is introduced between the strip and the wire, that activates only when the wire is in contact with the strip. The contact force is then computed as:

$$\begin{cases} F_c = k_c\left(x_{strip} - w(x_p.t)\right) & if\ x_{strip} > w(x_p.t) \\ F_c = 0 & otherwise \end{cases} \tag{4}$$

where $k_c$ is the contact stiffness (set to a value high enough to avoid significant penetration but not too high to cause numerical issues), $x_{strip}$ is the vertical position of the collector strip, and $w(x_p, t)$ is the vertical position of the contact wire at the longitudinal coordinate of the pantograph $x_p$.

## 2.4 PANTOHEALTH simulation engine

The PANTOHEALTH simulation engine implements the formulation described above in an integrated framework, which is able to simulate one or more pantographs running on long catenary section (up to several thousand of kilometers) at high speed. The numerical integration is performed, which is implicit and unconditionally stable for the structural part, while the contact and dropper non-linearities are solved at each time step with sub-iterations. The engine has been validated against the EN 50318 reference case [13] and against field measurements on real lines. In this paper, we used PANTOHEALTH version 3.0.0 to simulate four pantographs running on a two-section catenary with overlap, that is described in the next section.

## 2.5 Catenary System

The catenary system selected as test bench is a two-section system with one overlap area between the sections. The choice of relatively short catenary is motivated by the main objective of the paper, which is the investigation of the dynamic behavior in the overlap region, where the four pantographs are passing one after the other. Using a longer catenary would increase the simulation time without adding significant information for our analysis. Each section of the catenary has 10 spans with the span length varying between 47.98 m and 62.98 m, which are typical values for the European high speed catenary. The total length of one section is about 560 m and the overlap region is realized by superposition of last two spans of section 1 with first two spans of section 2.
Three different overlap profiles, denoted as Profile 1, Profile 2 and Profile 3, were designed and analyzed. The three profiles differ each other in two main aspects: (i) the position of droppers in the overlap region, in particular how many droppers are located in the transition spans and where they are located; (ii) the height of contact wire at the supports inside the overlap region, that determine the inclination of the contact wire when it leaves the in-service position and goes to the parked position (and viceversa for the other section). The three profiles are described in detail in the following.

Figure 1 compares the contact wire height (CWH) along the overlap region for the three profiles. Outside the overlap, the three profiles share the same nominal CWH of 5.3 m, and they also share the same dropper layout in the standard spans. The differences are concentrated at masts M9, M10 and M11, where the contact wire is progressively lifted from the in-service height of 5.3 m up to the parked position, and on the symmetric side of the second section. Profile 1 (blue) follows the standard arrangement, with intermediate heights of 5.45 m at M9 and 5.8 m at M10, and a parked height of 6.2 m at M11. Profile 2 (red) is very close to Profile 1, the only difference being a slightly higher value at M9 (5.5 m instead of 5.45 m); the parked height at M11 remains 6.2 m. Profile 3 (black dashed) is the most distinct of the three, because both the intermediate heights (5.4 m at M9 and 5.7 m at M10) and the parked height (6.1 m at M11) are reduced. The overall effect is a smoother transition from in-service to parked position: the average slope of the contact wire in the overlap drops from about 0.7–0.85% for Profile 1 and Profile 2 to about 0.65% for Profile 3. A smaller slope is expected to give less vertical excitation of the pantograph head when it enters and leaves the overlap, so the hypothesis is that Profile 3 will produce the smallest standard deviation of contact force, especially for the trailing pantographs. The simulation results in the next section confirm this expectation.

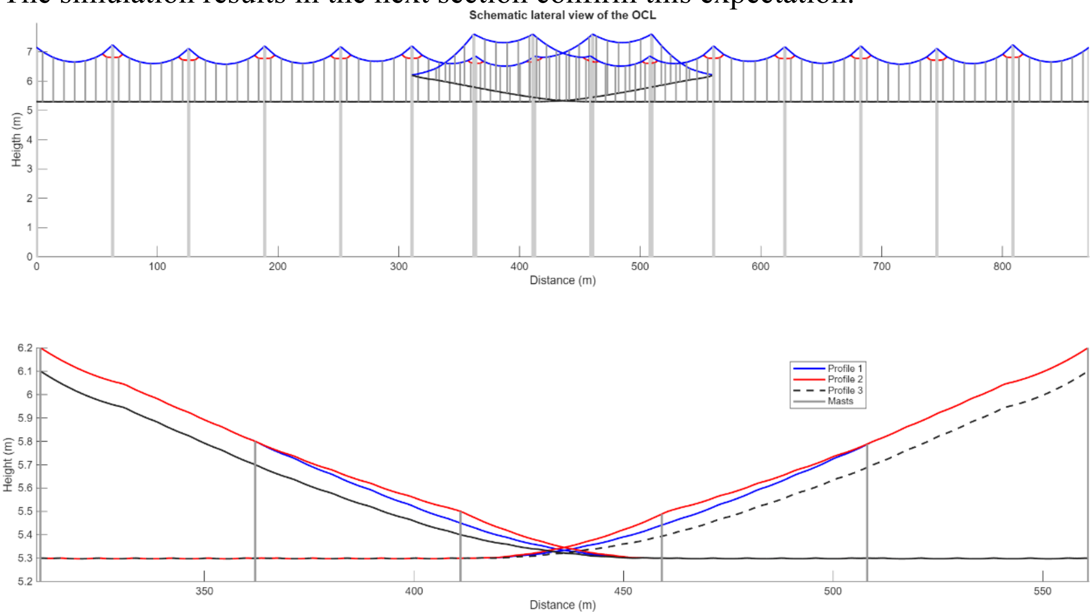


Figure 1: Contact wire height along the overlap region for the three profiles. Profile 1 (blue) and Profile 2 (red) reach a parked height of 6.2 m at M11, while Profile 3 (black dashed) adopts a reduced parked height of 6.1 m and slightly lower intermediate heights at M9 and M10.

## 3. Simulation results

The three overlap profiles described in Section 2 were simulated in PANTOHEALTH considering four pantographs in series, running over the two-section catenary with one overlap. For the present analysis, the distance between consecutive pantographs is first set to d1=d2=d3=192 m, but the case of multiple units with longer distance will be addressed in the second part of this section. Five operating speeds were analysed:

250, 275, 300, 325 and 350 km/h, that cover the typical range of European high-speed services. For each combination of profile and speed, the standard deviation of contact force is computed for each of the four pantographs, and the contact force distribution is presented in box plot.

Figure 2 shows the standard deviation of contact force versus operating speed for the four pantographs and the three overlap profiles. The first general observation is that for all three profiles and all four pantographs, the standard deviation increases with the operating speed, which is a well known fact in pantograph-catenary interaction. However, the rate of increase is not the same for all the pantographs.

Looking at Pantograph 1 (the leading pantograph), we see that the standard deviation is more or less the same for all three profiles, and it remains below 40 N for all the analysed speeds. This is expected because the leading pantograph operate on a catenary which is not yet perturbed by other pantographs, and the influence of the overlap design is limited because the overlap is just a part of the line and Pantograph 1 passes through it only once.

The situation is very different for Pantograph 2, 3 and 4. These trailing pantographs operate on a catenary which is already in vibration because of the passage of the previous pantographs. As we can see from Figure 2, the standard deviation of contact force for the trailing pantographs is significantly higher than the leading one, and it grows much faster with the speed. At 275 km/h, the three profiles show similar value with all pantographs producing standard deviation between 25 and 47 N. However, at 275 km/h, Profile 3 has the most consistent behaviour, with all four pantographs having standard deviation below 47 N, and Pantograph 1 even shows the smallest value of 22 N. This speed (275 km/h) seems to be a "sweet spot" for the system, where the wavelength of the catenary vibration is in resonance condition with the distance between pantographs in a way that minimize the disturbance.

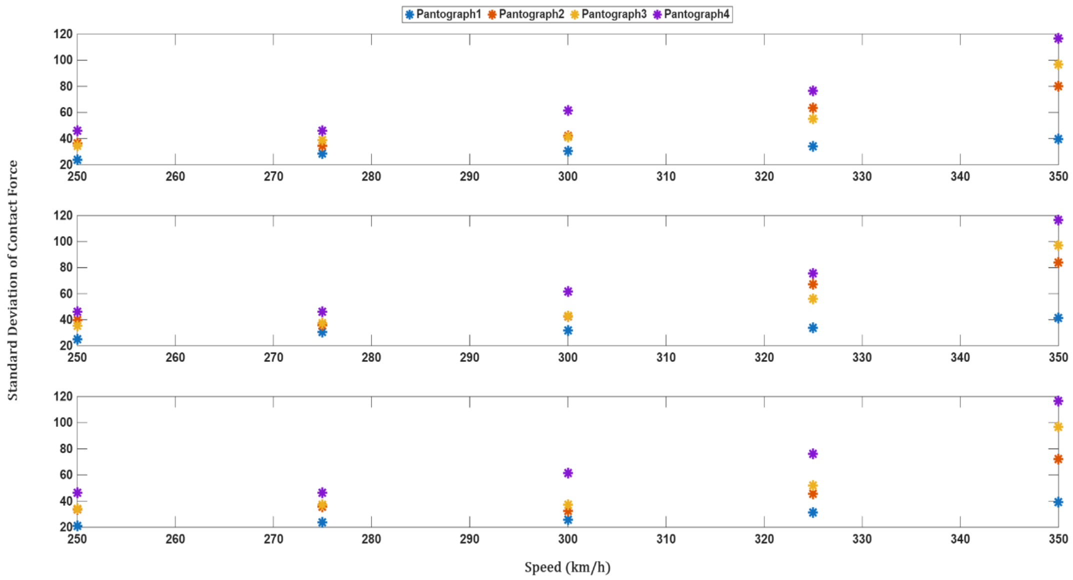


Figure 2: Standard deviation of contact force versus operating speed for the four pantographs (top: Profile 1, middle: Profile 2, bottom: Profile 3).

To complement the standard deviation analysis, the box plot of the contact force distribution at the five operating speeds was generated for each profile and each pantograph. Figures 5, 6 and 7 show respectively the box plot for Profile 1, Profile 2 and Profile 3. In each figure, the four sub-panels correspond to the four pantographs (from Pantograph 1 at the top to Pantograph 4 at the bottom). For each pantograph and each speed, the box represents the interquartile range of the contact force (25th to 75th percentile), the orange horizontal line is the median, and the whiskers extends to the minimum and the maximum values (excluding outliers).

For Profile 1 (Figure 5), the box plot of Pantograph 1 shows a quite compact distribution with the median around 130–180 N and the whiskers between 50 N and 250 N (depending on the speed). The distribution become wider when the speed increases, but it remains controlled. For Pantograph 2, 3 and 4, the box become much larger, and the minimum value of the whisker reach almost at 350 km/h. A contact force close to zero indicates loss of contact, which is critical condition that need to be avoided. We can see from Profile 1 that loss of contact occurs at 300 and 350 km/h for the trailing pantographs.

Profile 2 (Figure 6) shows a similar pattern as Profile 1. The Pantograph 1 distribution is reasonably compact, and the trailing pantograph distribution widen considerably at high speed. Comparing Pantograph 4 of Profile 2 with the same of Profile 1, the distribution is slightly more compact in Profile 2 at 250 and 275 km/h, but at 300, 325 and 350 km/h the two profiles produce essentially similar result.

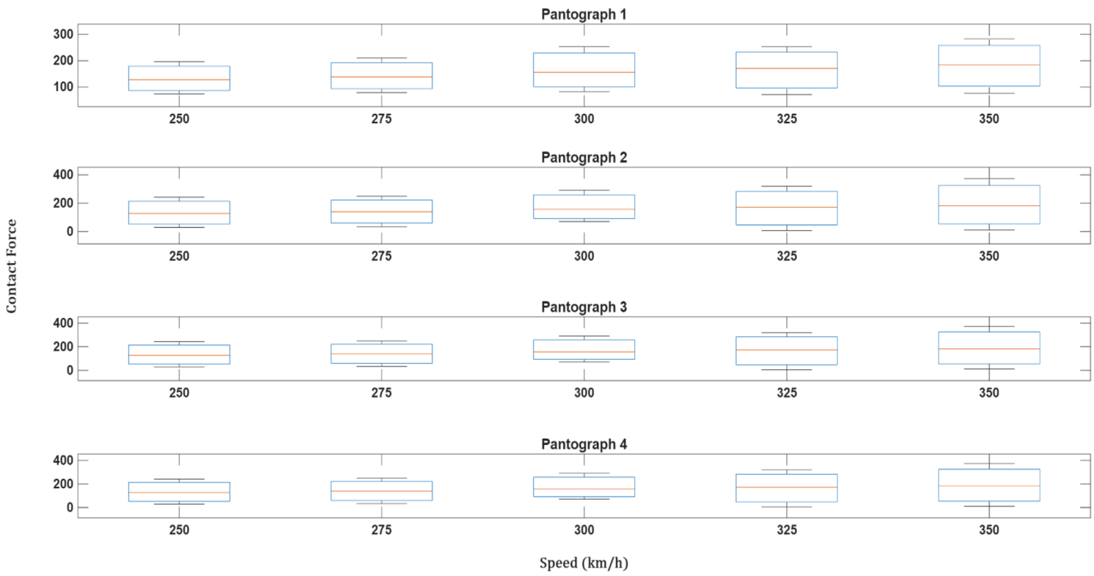


Figure 5: Contact force distribution at five operating speeds – Profile 1.

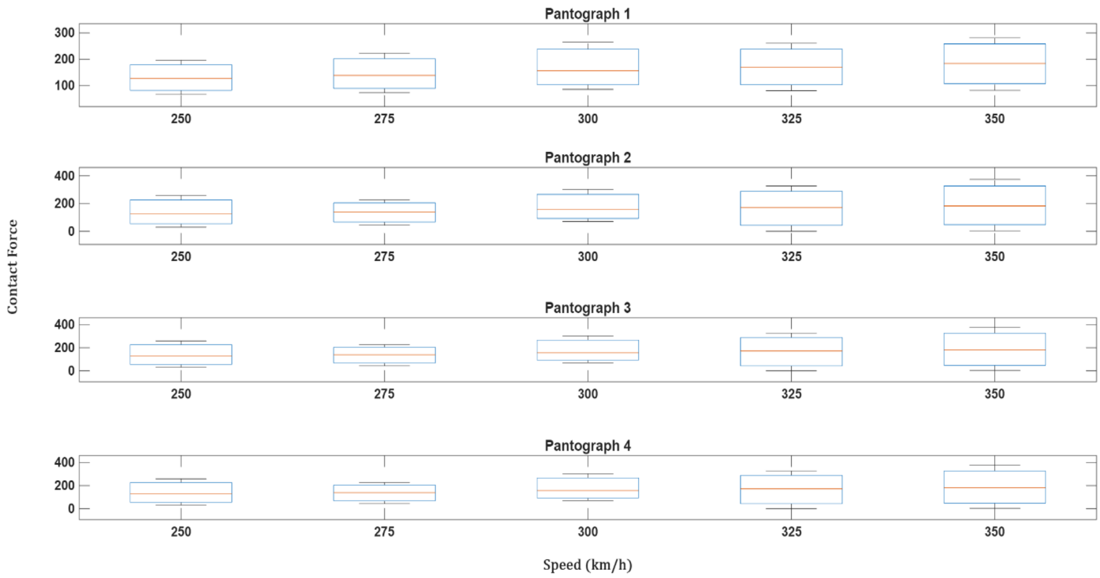


Figure 6: Contact force distribution at five operating speeds – Profile 2.

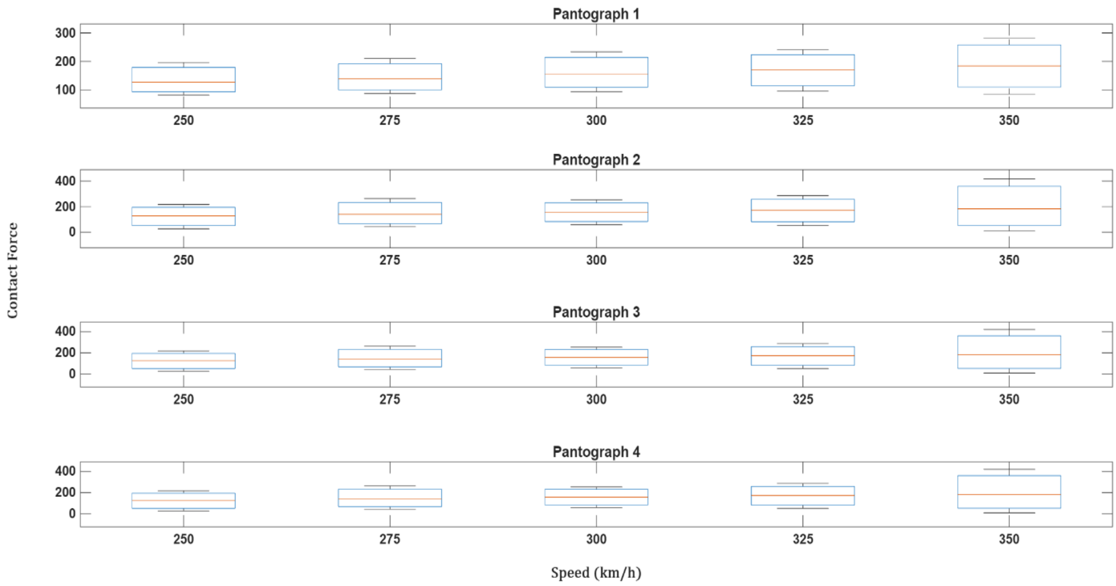


Figure 7: Contact force distribution at five operating speeds – Profile 3.

Profile 3 (Figure 7) is clearly the best of the three. The Pantograph 1 distribution stay between 80 N and 250 N for all the speeds, with the median close to 150 N. The Pantograph 2 distribution is also more compact, with smaller whiskers and the minimum value above zero in all cases (except at 350 km/h, where it touch zero). Pantograph 3 and Pantograph 4 show wider distributions, but the box (interquartile range) is smaller than Profile 1 and 2, especially at 275 km/h, where the box of Pantograph 3 is the smallest of all the three profiles. This confirms that Profile 3 gives the best balance between the four pantographs at the medium speed of 275 km/h.

Based on the standard EN 50318:2018 the standard deviation of contact force σ should be below a limit value that depends on the operating speed. For the speed considered in this work (around 275 km/h), the limit value of σ is approximately $0.3 \times F_m$, where

$F_m$ is the mean contact force. Considering $F_m$ in the order of 110–140 N, the limit value of σ is approximately 33–42 N. For the present analysis, we use a reference limit of $\sigma_{lim} \approx 38$ N for assessment.
Beside the standard deviation of contact force, two additional indicators are useful to evaluate the dynamic behaviour of the system in the overlap region. The first one is the maximum uplift of the contact wire at the support, shown in Figure 3 for the three profiles. The uplift at the support is an important parameter from the design point of view, because the standard EN 50119 limits the maximum allowed uplift in order to avoid mechanical damage of the registration arm and of the steady arm. Figure 3 indicates that the maximum uplift at the support grows with the operating speed for all four pantographs and for all three profiles, which is consistent with the increase of the standard deviation of contact force already observed in Figure 2. For Profile 1 (top panel) and Profile 2 (middle panel) the maximum uplift is essentially the same, and the trailing pantographs reach the highest values at 350 km/h. Profile 3 (bottom panel) shows slightly smaller values in the speed range 275–325 km/h, in particular at 275 km/h, where the uplift of all four pantographs stay grouped together. This confirms that the smoother contact wire transition of Profile 3 reduces also the uplift demand at the supports.

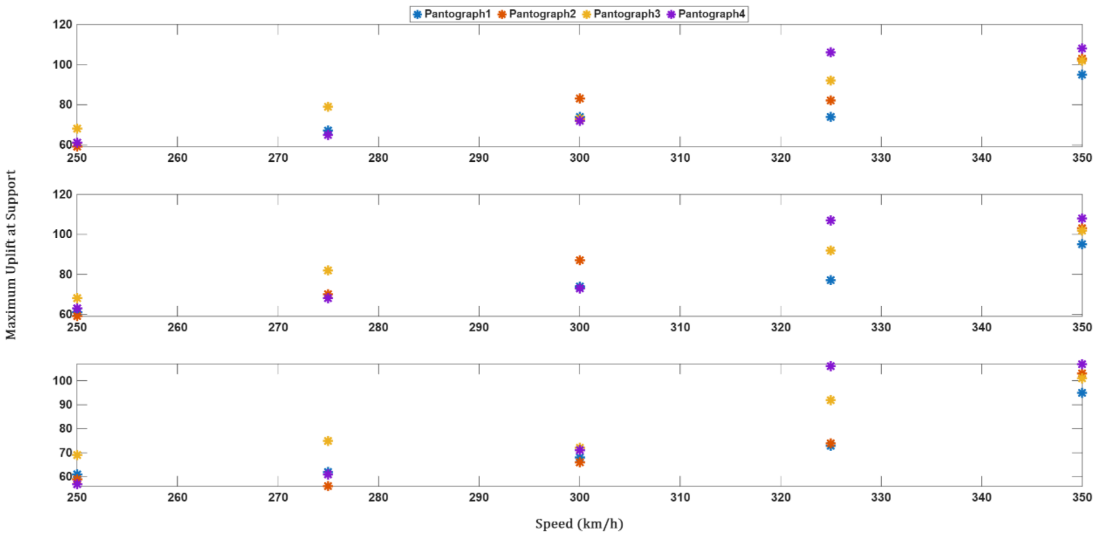


Figure 3: Maximum uplift of the contact wire at the support versus operating speed for the four pantographs (top: Profile 1, middle: Profile 2, bottom: Profile 3).

The second indicator is the vertical displacement range of the pantograph head, that is the difference between the maximum and the minimum vertical position of the collector strip during the passage of the pantograph over the catenary. A large displacement range means that the pantograph head is strongly excited by the catenary, which can produce loss of contact and increase the wear of the collector strip. Figure 4 shows the vertical displacement range of the four pantographs for the three profiles. As expected, the displacement range of the leading pantograph (Pantograph 1) is the smallest one and stay below 80 mm even at 350 km/h, while the trailing pantographs show much larger values. Pantograph 4 reaches the highest values at 350 km/h, which is close to three times the displacement range of Pantograph

1 at the same speed. Comparing the three profiles, the three panels show very similar patterns, which means that the displacement range is mainly driven by the operating speed and by the position of the pantograph in the consist, rather than by the small geometric differences between the profiles.

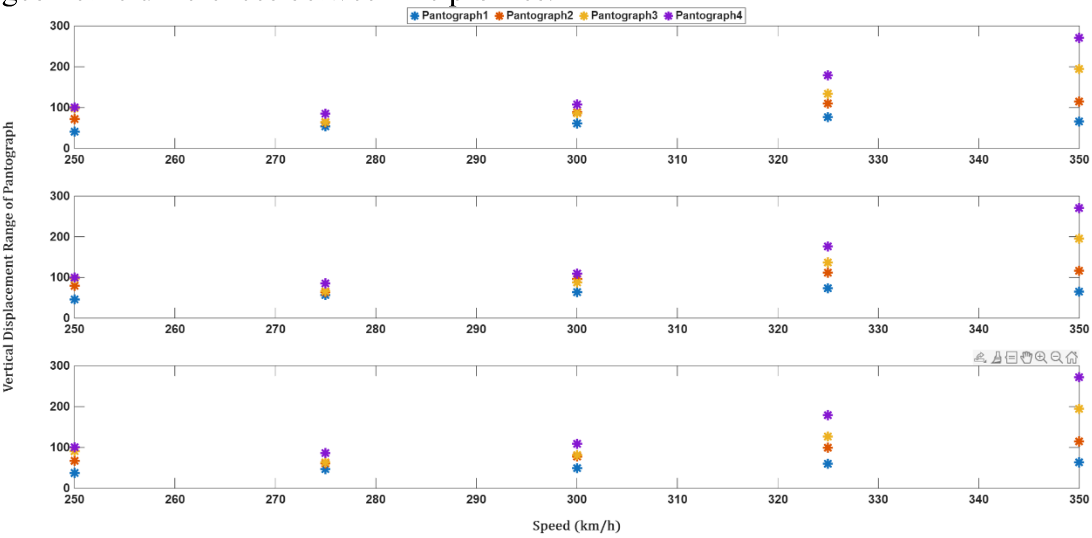


Figure 4: Vertical displacement range of the pantograph head versus operating speed for the four pantographs (top: Profile 1, middle: Profile 2, bottom: Profile 3).

The distance between Pantographs is varied in order to find the configuration that gives the best contact force quality for all the four pantographs. Considering the wavelength, twelve scenarios were defined to explore different combinations of distances d1 (between Pantograph 1 and 2), d2 (between Pantograph 2 and 3) and d3 (between Pantograph 3 and 4). Analysing Table 1, several important observations can be made. First, the standard deviation of Pantograph 1 ($\sigma p1$) is essentially constant across all the scenarios, with values in the narrow range 23.48–27.44 N. This is in agreement with what was already discussed before: the leading pantograph is not affected by the position of the other pantographs and its contact force quality depends only on the catenary itself.

Second, the trailing pantographs (Pantograph 2, 3 and 4) show large variation of standard deviation depending on the distance scenario. The worst case is Scenario 4 (uniform distance 152 m), where Pantograph 4 reaches 55.92 N, which is well above the limit of 38 N. The reason is that 152 m is approximately 2.5 times the span length (60 m), so the wave generated by Pantograph 1 arrives in phase at Pantograph 4 and constructive interference occurs. Scenarios 3, 5 and 12 also show very poor performance for the trailing pantographs, with values largely above 38 N.

Third, the scenarios that fully comply with the reference limit of 38 N for all the four pantographs are Scenario 1, Scenario 7, Scenario 8, Scenario 9 and Scenario 11. Among these, Scenario 1 (d1=d2=d3=120 m) gives uniform distance of 2 spans (approximately) and produce low standard deviation for all four pantographs (27.44, 32.56, 31.26, 30.85 N). Scenario 7 (d1=d2=d3=192 m) is on the borderline ($\sigma p3$=36.72 N) but still acceptable. Scenario 9 (d1=192, d2=120, d3=192 m) is

particularly interesting because the non-uniform distance configuration gives a very low standard deviation for Pantograph 3 (31.61 N) and Pantograph 4 (32.83 N), although Pantograph 2 is at 37.3 N (still below the limit, but close to it).
Scenarios 2, 3, 4, 5, 6, 10 and 12 do not comply with EN 50318 for at least one of the four pantographs. In particular Scenario 4 (152 m) and Scenario 12 (216 m) are the worst, with multiple pantographs exceeding the limit of 38 N by significant amount. These configurations should be avoided in the design phase. From the comparison of all the twelve scenarios, the best configuration is Scenario 9 (d1=192 m, d2=120 m, d3=192 m), where all four pantographs have σ ≤ 38 N and three of them (Pantograph 1, 3 and 4) are well below 35 N. This non-uniform distance configuration, combined with the optimized overlap of Profile 3 and the operating speed of 275 km/h, can be considered as the optimal design point identified by the present simulation campaign.

| Scenario | d1 [m] | d2 [m] | d3 [m] | σp1 [N] | σp2 [N] | σp3 [N] | σp4 [N] |
|---|---|---|---|---|---|---|---|
| 1 | 120 | 120 | 120 | 27.44 | 32.56 | 31.26 | 30.85 |
| 2 | 136 | 136 | 136 | 24.76 | 37.45 | 40.89 | 42.83 |
| 3 | 144 | 144 | 144 | 23.48 | 39.78 | 46.41 | 47.04 |
| 4 | 152 | 152 | 152 | 24.23 | 43.34 | 54.16 | 55.92 |
| 5 | 168 | 168 | 168 | 23.60 | 36.92 | 46.59 | 53.93 |
| 6 | 184 | 184 | 184 | 24.27 | 35.11 | 37.94 | 38.48 |
| 7 | 192 | 192 | 192 | 23.90 | 35.66 | 36.72 | 33.63 |
| 8 | 184 | 120 | 184 | 24.41 | 37.10 | 32.71 | 34.40 |
| **9** | 192 | 120 | 192 | 23.85 | 37.30 | 31.61 | 32.83 |
| 10 | 200 | 184 | 200 | 23.84 | 40.29 | 38.95 | 33.39 |
| 11 | 200 | 120 | 200 | 23.79 | 42.14 | 34.27 | 35.17 |
| 12 | 216 | 216 | 216 | 23.96 | 41.56 | 50.50 | 49.31 |

Table 1: Standard deviation of contact force for the twelve distance scenarios (Profile 3, V = 275 km/h). Green cells indicate compliance with the $\sigma_{lim}$ ≈ 38 N reference limit; orange cells indicate non-compliance.

The maximum uplift of the contact wire at the support was also examined for the twelve distance scenarios, in order to verify that the optimal configurations identified by the standard deviation analysis do not produce excessive uplift. Figure 8 shows the maximum uplift at the support for the four pantographs across the twelve scenarios, at Profile 3 and V = 275 km/h. The leading pantograph (Pantograph 1, blue) stays in a narrow band of about 60–64 mm in all the scenarios, which confirms that it is not affected by the position of the other pantographs. For the trailing pantographs the spread is much larger, with values that range from about 55 mm up to 112 mm. The worst case is Scenario 4 (uniform distance 152 m), where Pantograph 4 reaches about 112 mm and Pantograph 3 about 100 mm; this is consistent with what was already observed for the standard deviation, and it confirms that Scenario 4 should be avoided. Scenarios 3 and 12 also show high values for the trailing pantographs (above 90 mm and 75 mm respectively), in line with their non-compliance in terms of standard deviation. On the contrary, the compliant scenarios identified before (1, 7, 8, 9 and 11) show moderate uplift values: in Scenario 1 and Scenario 11 in particular, the four pantographs are grouped in a band of about 60–70 mm. Scenario 9 (d1 = 192 m, d2 = 120 m, d3 = 192 m), which gives the best contact force quality, shows maximum uplift below 75 mm for all four pantographs, well within the limits prescribed by EN 50119. This confirms that the optimal configuration is conservative also from the uplift point of view.

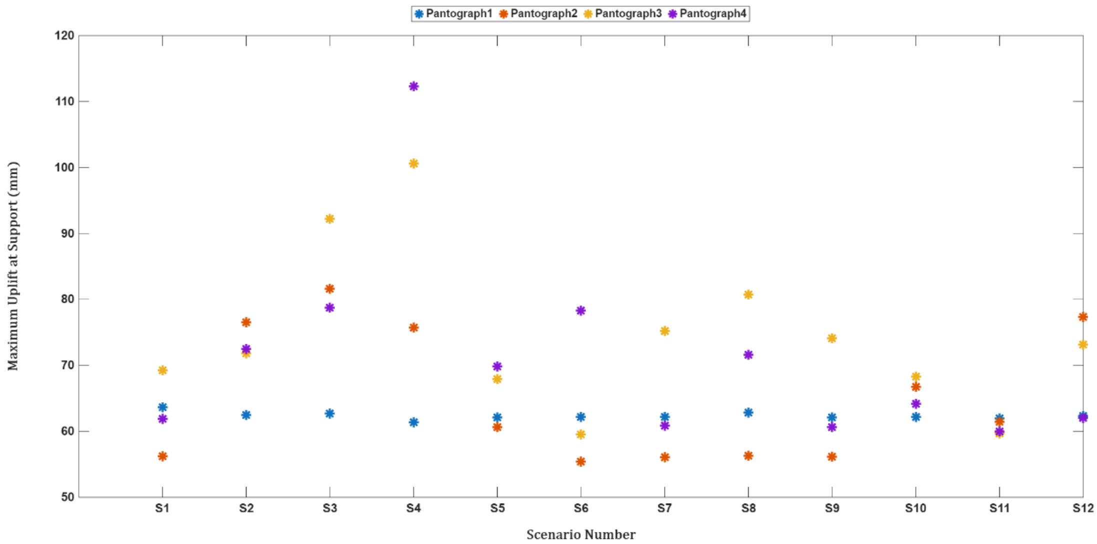


Figure 8: Maximum uplift of the contact wire at the support for the four pantographs across the twelve distance scenarios (Profile 3, V = 275 km/h).

## 4. Conclusions

In this paper, the dynamic interaction between four pantographs and a two-section catenary with one overlap has been investigated by means of numerical simulation using PANTOHEALTH simulation engine. Three different overlap profiles were designed and analysed at five operating speeds, and twelve distance scenarios between pantographs were tested in order to find the configuration that comply with the EN 50318 standard.

The main results obtained can be summarized as follow:

(1) The overlap geometry has significant effect on the contact force quality, especially for the trailing pantographs. A small modification of the contact wire height at the supports in the overlap region (from 5.45 m to 5.4 m at M9, from 5.8 m to 5.7 m at M10, and from 6.2 m to 6.1 m at M11, as it has been done in Profile 3) can reduce the slope of the contact wire and provide better dynamic behaviour.

(2) Among the three studied profiles, Profile 3 gives the best overall behaviour. The smaller transition step at the overlap area help to limit the excitation of the pantograph head and reduce the standard deviation of contact force for the trailing pantographs.

(3) The operating speed of 275 km/h is identified as the best speed for the analyzed catenary system. At this speed all four pantographs show low and uniform standard deviation, which is good for the wear of contact wire and for the maintenance of the pantograph head.
(4) Concerning the distance between pantographs, the non-uniform configuration of Scenario 9 (d1=192 m, d2=120 m, d3=192 m) gives the best compliance with EN 50318: all four pantographs have standard deviation below 38 N at the speed of 275 km/h with Profile 3. The non-uniform distance is more effective than the uniform distance for decoupling the dynamic of the four pantographs. The analysis of the maximum uplift at the support across the twelve scenarios confirms that this optimal configuration is conservative also from the structural point of view, with uplift values well below the limits prescribed by EN 50119, while the non-compliant scenarios (in particular Scenario 4) produce uplift values up to about 112 mm that would be critical for the supports.
Future work will be dedicated to extend the analysis to longer catenary (more than 2 sections), to include the effect of stochastic variability of catenary parameters (dropper length, contact wire pre-sag, support stiffness), and to investigate the influence of the train aerodynamic in the case of more than four pantographs operating together. Also, the comparison with field measurements is planned, in collaboration with a railway operator, in order to validate the conclusions obtained from the simulation.

## REFERENCES

[1] Bruni S., Ambrosio J., Carnicero A., Cho Y.H., Finner L., Ikeda M., Kwon S.Y., Massat J.P., Stichel S., Tur M., Zhang W., "The results of the pantograph-catenary interaction benchmark", Vehicle System Dynamics, vol. 53, no. 3, pp. 412–435, 2015.
[2] Ambrosio J., Pombo J., Pereira M., Antunes P., Mosca A., "A computational procedure for the dynamic analysis of the catenary-pantograph interaction in high-speed trains", Journal of Theoretical and Applied Mechanics, vol. 50, no. 3, pp. 681–699, 2012.
[3] Pombo J., Ambrosio J., "Multiple pantograph interaction with catenaries in high-speed trains", Journal of Computational and Nonlinear Dynamics, vol. 7, no. 4, 041008, 2012.
[4] Liu Z., Jönsson P.A., Stichel S., Rønnquist A., "On the implementation of an auxiliary pantograph for speed increase on existing lines", Vehicle System Dynamics, vol. 54, no. 8, pp. 1077–1097, 2016.
[5] Song Y., Liu Z., Wang H., Lu X., Zhang J., "Nonlinear analysis of wind-induced vibration of high-speed railway catenary and its influence on pantograph-catenary interaction", Vehicle System Dynamics, vol. 54, no. 6, pp. 723–747, 2016.
[6] Song Y., Liu Z., Ronnquist A., Navik P., Liu Z., "Contact wire irregularity stochastics and effect on high-speed railway pantograph-catenary interactions",

IEEE Transactions on Instrumentation and Measurement, vol. 69, no. 10, pp. 8196–8206, 2020.
[7] Bautista A., Montesinos J., Pintado P., "Dynamic interaction between pantograph and rigid overhead lines using a coupled FEM-multibody procedure", Mechanism and Machine Theory, vol. 97, pp. 100–111, 2016.
[8] Massat J.P., Laine J.P., Bobillot A., "Pantograph-catenary dynamics simulation", Vehicle System Dynamics, vol. 44, suppl. 1, pp. 551–559, 2006.
[9] Zhang W., Liu Y., Mei G., "Evaluation of the coupled dynamical response of a pantograph-catenary system: contact force and stresses", Vehicle System Dynamics, vol. 44, no. 8, pp. 645–658, 2006.
[10] Tan X., Lu Y., Liu Z., Song Y., "A machine learning based prediction method for pantograph-catenary system contact force", IEEE Transactions on Intelligent Transportation Systems, vol. 23, no. 7, pp. 8763–8773, 2022.
[11] Vesali F., Rezvani M.A., Molatefi H., Hecht M., "Static form-finding of normal and defective catenaries based on the analytical exact solution of the tensile Euler-Bernoulli beam", Proceedings of the Institution of Mechanical Engineers, Part F: Journal of Rail and Rapid Transit, vol. 233, no. 7, pp. 691–700, 2019.
[12] Vesali F., Molatefi H., Rezvani M.A., "Investigation on the influence of the catenary irregularities on the pantograph-catenary interaction", Journal of Theoretical and Applied Mechanics, vol. 56, no. 4, pp. 1097–1108, 2018.
[13] Vesali F., "Modelling and analysis of high-speed railway pantograph-catenary system dynamic interaction", Ph.D. Thesis, Iran University of Science and Technology, 2020.
[14] Cho Y.H., Lee K., Park Y., Kang B., Kim S.Y., "Influence of contact wire pre-sag on the dynamics of pantograph–railway catenary", International Journal of Mechanical Sciences, vol. 52, no. 11, pp. 1471–1490, 2010.